Isolation and Characterization of Vibrational Spectra of Individual Heme Active Sites in Cytochrome bc_1 Complexes from *Rhodobacter capsulatus*†

F. Gao,‡ H. Qin,§ M. C. Simpson,|| J. A. Shelnutt,|| D. B. Knaff,§ and M. R. Ondrias*,‡

Department of Chemistry, University of New Mexico, Albuquerque, New Mexico 87131, Department of Chemistry and Biochemistry, Texas Tech University, Lubbock, Texas 79409-1061, and Fuel Science Department, Sandia National Laboratories, Albuquerque, New Mexico 87185

Received February 21, 1996; Revised Manuscript Received June 4, 1996⊗

ABSTRACT: Resonance Raman spectra of bc_1 complexes and isolated c_1 subunit from *Rhodobacter capsulatus* have been obtained using a variety of excitation wavelengths. Spectra obtained via Q-band excitation of bc_1 complexes in different redox states were separated to yield the individual vibrational spectra of each of the three heme active sites. Hemes b_H and c_1 exhibit vibrational spectra typical of *b*- and *c*-type hemes, respectively. In contrast, the spectrum of heme b_L is anomalous with respect to those of other hemes *b*. The isolated spectra were also used to assess the effects of inhibitor binding on the local structural environments of the hemes. Neither antimycin nor myxothiazol binding produces dramatic structural perturbations at the hemes. Heme c_1 is completely unaffected by the presence of either inhibitor. The vibrational spectra of hemes b_H and b_L are slightly altered by antimycin and myxothiazol binding, respectively.

The cytochrome bc_1 complexes (complex III, ubiquinol−cytochrome *c* oxidoreductase) comprise a superfamily of integral membrane proteins which play pivotal roles in the electron transport chains of mitochondria, chloroplasts, and bacteria (Knaff, 1993; Hauska et al., 1983; Brandt & Trumpower, 1994). All bc_1 complexes contain a core of three redox-active proteins (Brandt & Trumpower, 1994), harboring a total of four redox-active sites (three hemes and one FeS cluster). The bc_1 complexes used in this study are isolated from the photosynthetic purple bacterium *Rhodobacter capsulatus*. These complexes are structurally, spectroscopically, and functionally similar to their mitochondrial counterpart but have only three subunits (as opposed to 9−11 subunits in the mitochondrial bc_1 complex). This greatly simplifies both the protein chemistry and genetic manipulation of the bacterial complexes (Knaff, 1993; Gray et al., 1992; Gennis et al., 1993; Davidson et al., 1992).

Cytochrome bc_1 complexes perform multiple functions. They catalyze the flow of electrons from a quinol to a soluble redox protein (either a *c*-type cytochrome or, in the case of the related cytochrome b_6f complex, a plastocyanin) and couple the exogenicity of this electron transfer to proton translocation across the membrane in which the complex is imbedded (Knaff, 1993). The mechanisms of these processes have been the subjects of intense scrutiny over the past three decades and can be both qualitatively and quantitatively understood in term of the modified Q-cycle model [see, for example, Crofts and Wang (1989), Trumpower (1990) Mitchell (1976) and Brandt and Trumpower, (1994)]. The Q-cycle model (Figure 1) postulates a branched electron transfer pathway with two separate substrate binding sites: Q_o, the quinol oxidation site, and Q_i, the quinone reduction site. The sequential oxidation of two quinols occurs at the Q_o site near the iron−sulfur cluster and a low potential heme b_L. The two electrons removed from each quinols at the Q_o site are gated into high- and low-potential chains of one-electron redox couples. The high-potential pathway through the FeS cluster and a *c*-type heme (cytochrome c_1) ultimately leads to reduction of a soluble cytochrome, while electrons transferred via the low-potential pathway through the two *b*-type hemes are utilized to regenerate quinol at the Q_i site.

During the past two decades, physical, biochemical, and spectroscopic investigations have done much to clarify the relative positions and general equilibrium structures of the four redox-active prosthetic groups of the bc_1 complexes. In bacterial bc_1 complexes (Yun et al., 1991, 1992; Robertson et al., 1994; Hobbs et al., 1990; Gray et al., 1992; Chen et al., 1995; Beattie et al., 1994), the cytochrome *b* subunit is composed of eight membrane-spanning helices and contains two inequivalent *b*-type (protoheme) hemes (Yun et al., 1991; Daldal et al., 1989) that differ in both E_m values and absorption spectra. These two hemes are usually designated by their redox potentials as heme b_H (high potential, $E_m = +40$ mV in R.c. bc_1)[1] and heme b_L (low potential, $E_m = -90$ mV). A single *c*-type heme ($E_m = +290$ mV) resides in the cytochrome c_1 subunit (Knaff, 1993; Davidson & Daldal, 1987). The iron−sulfur subunit contains a single 2Fe−2S (Rieske-type) iron−sulfur cluster. As the flow of electrons in the bc_1 complex requires the intimate participation of these active sites, knowledge of their equilibrium structures and possible long-range interactions is required

† This work was supported by the National Institutes of Health (GM 33330 to M.R.O.), the U.S. Department of Agriculture (93-37306-9084 to D.B.K.), the Robert A. Welch foundation (D-0710 to D.B.K.), the National Science Foundation (Shared Instrumentation Grant to the Texas Tech Biotechnology Institute), and the Department of Energy Distinguished Postdoctoral Research Program (M.C.S.).

‡ University of New Mexico.

§ Texas Tech University.

|| Sandia National Laboratories.

⊗ Abstract published in *Advance ACS Abstracts,* September 1, 1996.

[1] Abbreviations: MCD, magnetic circular dichroism; EPR, electron paramagnetic resonance; RR, resonance Raman; RRS, resonance Raman spectroscopy; RDS, Raman difference spectroscopy; R.c., *Rhodobacter capsulatus*; Cco, cytochrome *c* oxidase; ET, electron transfer; DMSO, dimethyl sulfoxide; $FePP(ImH)_2$, iron protoporphyrin bis(imidazole); Im^-, imidazolate.

S0006-2960(96)00419-9 CCC: $12.00

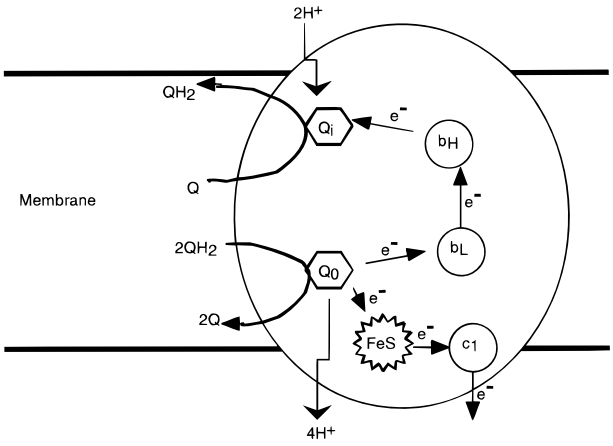

FIGURE 1: Schematic of the bc_1 complex modified Q-cycle mechanism. The membrane embedded protein has three heme prosthetic groups denoted by b_H, b_L, and c_1 (cycles), one iron−sulfur cluster shown as FeS (star). The postulated quinol oxidation site Q_0 and quinone reduction site Q_i are depicted as polygons. [Adapted from Gennis et al. (1993).]

for a complete mechanistic picture of electron transfer within this important energy-transducing complex.

In the absence of a crystal structure, only a general picture exists of the local structures of the heme active sites (Knaff, 1993) for bc_1 complexes. The specific amino acid side chains serving as ligands for the b_H and b_L hemes are four histidines (i.e., a pair of histidines serve as axial ligands for each heme). The results of near-infrared MCD (Finnegan et al., 1996; Simpkin et al., 1989), EPR (Carter et al., 1981), and mutagenesis studies (Yun et al., 1991; Hauska & Herrmann, 1988; Gennis et al., 1993) are all consistent with this assignment. Sequence comparisons across the family of cytochromes b (Yun et al., 1991) yield four conserved histidines (H97, H111, H198, and H212) which are obvious candidates for the heme b axial ligands. These residues occur within transmembrane helices II and IV of cytochrome *b* (Knaff, 1993). In order to accommodate heme ligation by the conserved histidines, these helices must be adjacent and parallel to each other and the hemes must lie in close proximity to each other within the same interhelical space (Gennis et al., 1993). However, the structural differences giving rise to the considerable variation in E_m between these hemes remain a subject of debate. Histidine/methionine axial ligation appears most likely for the heme *c* active site of cytochrome c_1 (Lou et al., 1993; Knaff, 1993; Gray et al., 1992). However, recent near-IR MCD evidence (Finnegan et al., 1996) suggests that a potential coordinating residue-(s) other than methionine is(are) sufficiently close to the heme c_1 to serve as an alternative axial ligand either when solvent perturbation occurs or in mutants in which the native methionine axial ligand has been replaced by a nonliganding amino acid.

The electron transfer functions of bc_1 complexes can also be affected by the binding of inhibitors. There are two sets of inhibitors which will block the electron transfer pathway within the bc_1 complexes (Slater, 1973; Link et al., 1993; Howell & Robertson, 1993; Gennis et al., 1993; Daldal et al., 1989). Antimycin, funiculosin, and related inhibitors block the reduction of the quinone and are thought to bind at or near the Q_i site, located near the heme b_H. Another set of inhibitors, including myxothiazol, stigmatellin, and UHDBT, blocks the oxidation of quinol and is presumed to bind at or near the Q_o site, proximal to heme b_L and the iron−sulfur cluster.

Long-range structural interactions can, in principle, alter the structure of active sites in mechanistically important ways. For instance, allosteric interactions play prominent roles in the function of hemoglobins (Rousseau & Friedman, 1988) and cytochrome *c* oxidase (Babcock, 1988). While the magnetic and optical spectra of the hemes in bc_1 complexes offer no indications of direct electronic coupling, some evidence does exist for long-range heme−heme interactions. For example, the binding of inhibitors to the Q_i and Q_o sites affects the absorption spectra (Kunz & Konstantinov, 1983; Howell & Robertson, 1993), EPR signals (McCurley et al., 1990), and redox potentials (Howell & Robertson, 1993) of the putative proximal heme (b_H and b_L, respectively). These perturbations are small but clearly indicate a reorganization of heme environments in response to inhibitor binding (Howell & Robertson, 1993). Evidence for even longer-range interactions can be found in the slight perturbation of the absorption spectra of the distal hemes induced by inhibitor binding. Redox cooperativity, if it exists at all, among the hemes has been shown to be less than 100 mV (Rich et al., 1990).

Resonance Raman spectroscopy (RRS) provides a direct means of assessing the structural characteristics of chromophores in proteins (Spiro & Li, 1988) and has been proven particularly effective in probing the local environments of hemes (most notably heme axial ligation and direct protein environment/heme interactions). For instance, the application of RRS to elucidate the equilibrium structures and structural dynamics of cytochrome *c* oxidase has aided immensely in producing a detailed reaction mechanism of the dioxygen reduction at the cytochrome a_3/Cu_B site (Babcock & Varotsis, 1993; Takahashi et al., 1994). The present study of the bc_1 complexes seeks to emulate the initial Cco studies (Babcock, 1988) by utilizing selective resonance enhancement to isolate the RR spectra of the b_H, b_L, and c_1 hemes. Once isolated, the individual heme spectra are used to characterize the effects of the binding of various ET inhibitors on the structures of the hemes.

MATERIALS AND METHODS

Rb. capsulatus bc_1 complexes were isolated according to the previously described methods (Gray et al., 1992; Güner et al., 1993). *Rb. capsulatus* cytochrome c_1 was separated from the bc_1 complex and purified as described previously (Finnegan et al., 1996; Gray et al., 1992). All purified protein samples were stored at 77 K until used. Antimycin and myxothiazol were purchased from Sigma Chemical Co. (St. Louis, MO). All other reagents were obtained from commercial sources and were the highest quality available.

The bc_1 purification protocol produces samples with a mixture of c_1 (+2/+3) redox states and were further treated to manipulate the net redox state of hemes. Fully oxidized (all ferric hemes), partially reduced [c_1(+2), b_H(+2/+3), and b_L(+3)] and fully reduced (all ferrous hemes) samples were prepared by the addition of minimal amounts of solid potassium ferricyanide, sodium ascorbate, and sodium dithionite, respectively, to solutions of bc_1 complexes buffered to a pH of 8.0 (in 50 mM Tris-HCl, 100 mM NaCl, and 0.1 mg/mL dodecyl maltoside solutions). Anaerobic conditions were employed for manipulation of the partially and fully reduced

samples. Samples for Raman spectroscopy were prepared by mixing stock solutions (20−25 μL) of protein (140−150 μM) with a minimal amount of solid reductant (sodium dithionite or sodium ascorbate) in sealed capillary tubes. Where applicable, inhibitors were mixed with stock samples using 1−3 μL of concentrated ethanol (or DMSO) solution immediately before they were transferred to the sample tubes and reduced. Control samples were made from identical solutions without the inhibitors and monitored to ensure that the addition of ethanol (DMSO) did not affect the bc_1 spectra under the experimental conditions employed. The strong 1:1 binding of antimycin to the complex was verified by absorption and luminescence quenching titrations (Slater, 1973) using a Perkin-Elmer Lambda 19 UV/vis/NIR absorption and a Perkin-Elmer LS-5 fluorescence spectrophotometer.

Resonance Raman spectra were obtained using a laser photonics UV24 nitrogen-pumped dye laser (tunable range 380−830 nm) via a backscattering geometry and dispersed in a Chromex 500IS spectrometer (Chromex, Albuquerque, NM) with a liquid nitrogen-cooled CCD detector (Princeton Instruments, Inc. LN/CCD). This system produced ∼10-ns pulses of 0.3−0.5 mJ/pulse at 10−15 Hz. Cylindrical lenses were used to focus the beam at the sample. Long-pass filters (CVI Laser, Albuquerque, NM) were used to remove the background scattering light from the sample where applicable. Raman spectra were processed with Chromsoft (version 2.31). Toluene and benzene were used for spectral calibration. Raman difference spectroscopy (RDS) was performed at Sandia National Laboratories with instrumentation described elsewhere (Shelnutt et al., 1981). Some of the spectral analyses were performed by using Grams/386 software (Galactic Industries Corp.).

RESULTS AND DISCUSSION

(I) Isolation of Heme Spectra

As all three hemes in bc_1 complexes are low-spin and six-coordinate (Finnegan et al., 1996), they exhibit qualitatively similar optical spectra. It is important to isolate the spectra of the individual hemes in order to further identify and characterize the local structure of the heme pockets and any structural changes occurring at these sites. Fortunately, the c_1, b_H, and b_L hemes exhibit widely separated reduction potentials. Thus, careful comparisons among bc_1 complexes prepared in different redox states can be used to deconvolute the net optical spectra.

(A) Absorption Spectra. Figure 2 shows the absorption spectra obtained from isolated ferrous and ferric c_1 subunits and bc_1 complexes in their oxidized [$b_L(+3)$, $b_H(+3)$, and $c_1(+3)$], ascorbate- ($E^{0'} = 58$ mV) reduced [$b_L(+3)$, $b_H(+3/+2)$, and $c_1(+2)$], and dithionite- ($E^{0'} = 527$ mV) reduced [$b_L(+2)$, $b_H(+2)$, and $c_1(+2)$] forms. Here the "fresh" ascorbate-reduced spectrum refers to the spectrum taken immediately after adding the reductant. The relatively narrow band at ∼552 nm indicates that only cytochrome c_1 is reduced at this stage. The "aged" spectrum was obtained 2 h after adding ascorbate. The shoulder at ∼560 nm in this spectrum is a clear indication of the partial reduction of the b_H heme. The qualitative effects of progressive reduction of the hemes in the bc_1 complex are readily seen in behavior of both the B-band (400−450 nm) and Q-band (500−600 nm) regions of the heme optical spectra. Iron reduction produces a general shift in the B-band to lower energy (red shift) and a dramatic increase in the oscillator strength of the Q_{00} and Q_{01} transitions at ∼555 and ∼525 nm, respectively. The combined spectra [$b_H(+2) + b_L(+2)$] can be obtained (see trace b of Figure 2, panel III) by subtraction of appropriate c_1 spectra from that of fully reduced complex. It is apparent from the difference spectrum that the *b*-hemes exhibit pronounced red shifts relative to heme c_1 for both sets of transitions. Further isolation of the spectra to obtain the individual b_H and b_L contributions in the B-band region is complicated by the presence of spectral contributions from all six heme species (ferric and ferrous). In the Q-band region, however, the ferrous hemes dominate the spectrum and the Q_{00} transitions of the ferrous hemes are distinct enough to extract their individual contributions to the composite band at 550−565 nm. Figure 2, panel IV shows the isolated Q_{00} bands for ferrous c_1, b_H, and b_L. Table 1 summarizes the results of the absorption spectrum deconvolution.

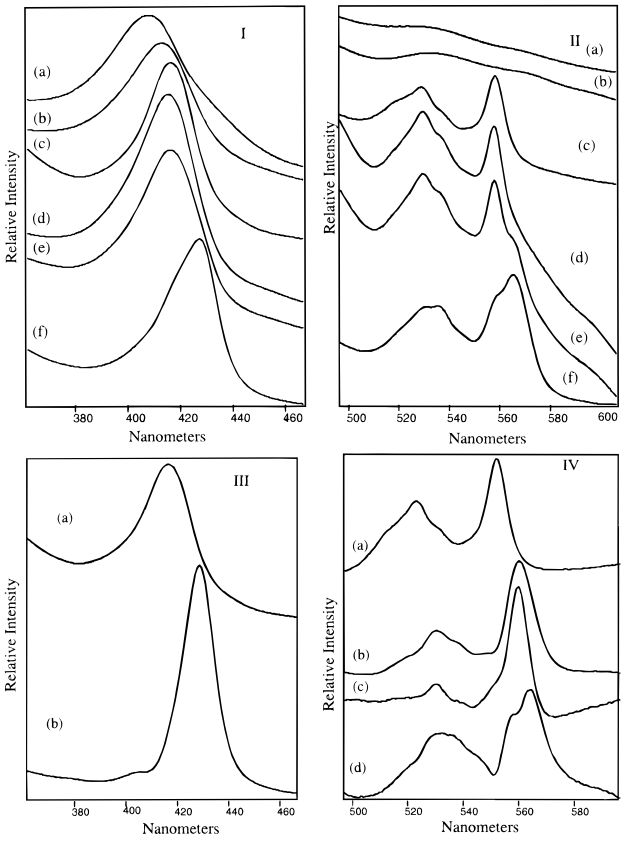

FIGURE 2: (Panels I and II) Absorption spectra of R.c. bc_1 complexes and isolated c_1 subunits. (I) B-band region of (a) ferric c_1 subunit, (b) ferric bc_1 complex, (c) ferrous c_1 subunit, (d) bc_1 complex immediately after addition of ascorbate, (e) bc_1 complex 2 h after ascorbate addition, and (f) ferrous bc_1 complexes reduced with dithionite. (II) Q-band region of the same samples as panel I. (Panels III and IV) Isolated absorption spectra of hemes. (III) B-band region of (a) isolated ferrous c_1 subunit, (b) b_H (ferrous) + b_L (ferrous) obtained by weighted subtraction of trace c from trace f in panel I. (IV) Q-band region: (a) and (b) from the same samples as in panel III, (c) ferrous b_H spectrum obtained by subtraction of trace d from trace e in panel II, and (d) ferrous b_L spectrum obtained by subtraction of trace c from trace b in this panel. bc_1 samples were ∼35 μM in 50 mM Tris-HCl, 100 mM NaCl, and 0.1 mg/mL (w/v) dodecyl maltoside, pH = 8.0. The c_1 sample was in 25 mM Tris-HCl (pH 8.0), 1 mM DTT, 1 mM EDTA, and 0.25% (w/v) cholate.

The distinct Q_{00} bands and widely different redox potentials of hemes b_H and b_L clearly indicate that their

Table 1: Q_{00} Absorption Spectra for Reduced Species of *Rb. capsulatus*

	B (nm)	Q_{00} (nm)	Q_{01} (nm)
c_1 (isolated)	416.4	551.9	523.1
c_1 (in bc_1)		551.7	523.3
$b_H + b_L$	428.5	560.2	530.5
b_H		559.9	
b_L		558.0, 564.5	

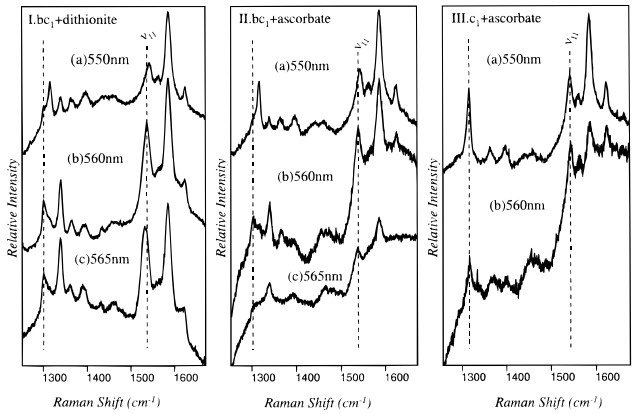

FIGURE 3: Q-band resonance Raman spectra of R.c. bc_1 complexes and isolated c_1 subunits. (I) Spectra of ferrous bc_1 complexes obtained with (a) 550-nm, (b) 560-nm, or (c) 565-nm excitation. (II) Spectra of ascorbate reduced bc_1 complexes (aged) at (a) 550-nm, (b) 560-nm, and (c) 565-nm excitation. (III) Spectra of ferrous c_1 subunits at (a) 550-nm or (b) 560-nm excitation. Sample preparation was the same as in Figure 2 with a protein concentration of ~150 μM. Laser power of ~8 mW at 10 Hz was used. Long wave pass filter SOG-570 (CVI Laser) was used with 550-nm excitation, and LP-580 long wave pass filter (CVI Laser) was used with 560- and 565-nm excitation to minimize background noise. Spectra were accumulated for 10−15 min at a spectral resolution of ~4 cm^{-1}.

local environments are quite different. The $\pi-\pi^*$ bands of cytochrome c_1 are typical of a *c*-type heme and are largely unaffected by dissociation of the cytochrome c_1 subunit from the rest of the complex. As a class, *b*-type hemes exhibit optical spectra that are red-shifted relative to *c*-type hemes (Otsuka & Yamanaka, 1988). The vinyl substituent of b-type hemes, due to its conjugation with the ring and its electron-withdrawing properties, contributes most to the red shift, but the His/His *vs* His/Met ligation may also affect the energies of the porphyrin transitions. In addition, both b_H and b_L exhibit inhomogeneously broadened bands. For b_L, the effect is quite pronounced, producing two distinct Q_{00} bands at 558 and 565 nm. A careful electrochemical/spectral study of the b-heme spectra of a mitochondrial cytochrome bc_1 complex by Howell and Robertson (1993) showed that the b_L behavior resulted from both the splitting of heme *x,y* degeneracy and the existence of at least two distinct local protein conformations. The putative *x,y* splitting in heme b_H is considerably less and no evidence was found for subpopulations. Nonetheless, the inhomogeneity displayed by both *b*-hemes suggests that both inhabit structurally flexible protein pockets.

(B) Resonance Raman Spectra. Resonance Raman spectra were obtained for bc_1 complexes in various redox states using both B-band (data not shown) and Q-band (Figure 3) excitation. Spectra obtained with 406-nm excitation (summarized in Table 2) are dominated by A-term scattering from polarized (A_{1g}) and depolarized (B_g) heme modes corresponding primarily to in-plane porphyrin ring vibrations (Hu et al., 1993). B-band spectra for the oxidized and reduced

Table 2: B-Band RR Modes for *Rb. capsulatus* c_1 and bc_1 Complexes

	ν_4 (cm^{-1})	ν_3 (cm^{-1})	ν_2 (cm^{-1})	ν_{10} (cm^{-1})
bc_1 oxidized	1375	1507	1584	1642
bc_1 reduced	1362	1494	1586	1619
c_1 oxidized	1375	1507	1586	1636
c_1 reduced	1362	1494	1585	1619

complexes are generally consistent with those obtained from low-spin six-coordinate hemes and closely resemble analogous spectra of bc_1 complexes from mitochondria and other bacterial sources (Hobbs et al., 1990). Unfortunately, as all three hemes exhibit very similar B-band transitions, the resonance enhancements of scattering from different hemes display little selectivity. Thus, resonance selectivity could not be employed to isolate the contributions from the individual hemes. Attempts to isolate the RR spectra obtained at a single excitation (406 nm), via subtraction protocols similar to those used above for absorption spectra, were significantly complicated by the fact that both ferric and ferrous hemes scatter efficiently with B-band excitation.

The distinct separation of the heme Q_{00} bands (Figure 2, panel IV) offers a far more promising means of isolating the vibrational spectra of the individual hemes. Q-band excitation enhances scattering from inversely polarized and depolarized modes via the Herzberg−Teller mechanism and thus yields spectra that complement those obtained via B-band excitation (Hu et al., 1993). In particular, the prominent modes at ~1305, 1315, 1340, 1540, and 1585 cm^{-1} correspond to B_g or A_{2g} symmetry modes that are absent or weakly present in B-band spectra. Figure 3 shows the dependence of the spectra of various bc_1 species upon excitation wavelength at the Q_{00} region (550−565 nm). In contrast to B-band excitation, only ferrous hemes exhibit appreciable absorbance in the 550−570-nm region and thus they are the only contributors to the resonance Raman spectra. Varying excitation wavelength through the Q-band has a dramatic effect on the positions and relative intensities of the observed composite spectra. Of particular interest are the trio of bands from 1300 to 1350 cm^{-1}, which can be used to quantify the relative contributions of heme c_1 and the *b* hemes (see below), and the ν_{11} band at ~1540 cm^{-1}, which is particularly sensitive to the nature of heme axial ligands (Othman et al., 1994; Lou et al., 1993; Hobbs et al., 1990; Desbois & Lutz, 1992). The strong band at ~1315 cm^{-1} in the 550-nm excitation spectra is diagnostic for thioether linkages at the heme periphery, while the presence of two bands at ~1300 and ~1340 cm^{-1} arises from a Fermi resonance between the ~1315-cm^{-1} porphyrin skeletal mode and the bending modes ($\delta_{(CH=)}$ and $\delta_{(=CH_2)}$) of the vinyl substituents of heme *b* (Lou et al., 1993; Kitagawa et al., 1977; Hobbs et al., 1990; Adar & Erecinska, 1974). The relative intensities of these modes in the composite spectra of bc_1 complexes show that spectra obtained with 550-nm excitation are dominated by scattering from heme c_1, while with 560- and 565-nm excitation, modes from the *b* hemes predominate (Table 3). Furthermore, the high S/N ratio and excitation wavelength dependence of the Q-band spectra permits their separation into the individual spectra of b_H, b_L, and c_1 (see Figure 4 caption for details). The results of this analysis are shown in Figure 4 and summarized in Table 3. These individual spectra clearly reveal significant structural differences among the c_1, b_H, and b_L hemes.

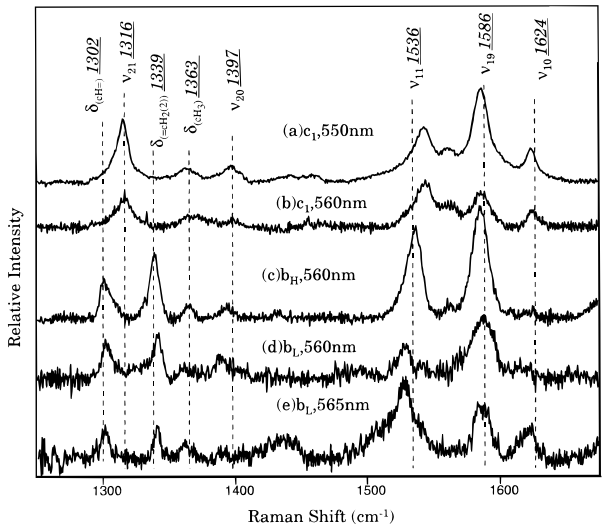

FIGURE 4: Isolated Q-band RR spectra (baseline-corrected) for ferrous bc_1 hemes (a) c_1 subunit (550 nm), (b) c_1 subunit (560 nm), (c) ferrous heme b_H spectrum (560 nm) obtained by the weighted subtraction of the ferrous c_1 subunit spectrum at 560 nm (Figure 3, trace b in panel III) from the ascorbate reduced (aged) bc_1 spectrum at 560 nm (Figure 3, trace b in panel II), (d) ferrous heme b_L spectrum (560 nm), obtained by subtracting both ferrous subunit c_1 (Figure 3, trace b in panel III) and ferrous heme b_H spectra (trace c, this figure) from the spectrum of the dithionite-reduced bc_1 complex (Figure 3, trace c in panel I), (e) ferrous heme b_L spectrum at 565-nm excitation obtained by subtracting the ascorbate-reduced bc_1 spectrum (Figure 3, trace c in panel II) from the dithionite-reduced bc_1 spectrum (Figure 3, trace c in panel I).

RR spectra of ferrous heme c_1 (Figure 4a) are generally similar to those of soluble cytochromes *c* (Lou et al., 1993; Kitagawa et al., 1977; Hobbs et al., 1990; Adar & Erecinska, 1974). The positions of the high-frequency modes are quite consistent with a low-spin six-coordinate heme site. Closer examination of the heme c_1 spectrum reveals some systematic differences between the heme of cytochrome c_1 and that of horse heart cytochrome *c*. These are most evident in the behavior of the heme core size-sensitive modes, ν_{11} and ν_{19}. Those modes (particularly ν_{11}) have been shown to be quite sensitive to the nature of the heme axial ligands in a wide variety of six-coordinate heme proteins (Othman et al., 1994; Lou et al., 1993; Kitagawa et al., 1977; Hobbs et al., 1990; Desbois & Lutz, 1992; Desbois, 1994; Adar & Erecinska, 1974). Qualitatively, the positions and relative intensities of ν_{11} and ν_{19} more closely resemble those of cytochrome *c* at neutral pH (His/Met ligation) (Othman et al., 1994; Lou et al., 1993; Kitagawa et al., 1977; Adar & Erecinska, 1974). However, the position of ν_{11} is downshifted by $\sim$4 cm^{-1}, while ν_{19} is slightly upshifted ($\sim$2 cm^{-1}) for R.c. c_1 ($\nu_{11} \sim$ 1543 cm^{-1}, $\nu_{19} \sim$ 1586 cm^{-1}) compared to cytochrome *c* ($\nu_{11} \sim$ 1547 cm^{-1}, $\nu_{19} \sim$ 1584 cm^{-1}). This at least partially reflects the heme pocket environmental differences between the R.c. c_1 and horse heart cytochrome *c*. Furthermore, spectra of heme c_1 obtained via subtraction of bc_1 spectra are almost identical to those obtained from isolated cytochrome c_1.

Spectra of fully reduced bc_1 complexes obtained with $\sim$560-nm excitation are consistent with the fundamental structural differences between hemes *b* and *c*. In general, *b*-hemes possess free vinyl groups (indicated by bands at $\sim$1300 and 1340 cm^{-1}) and nitrogen axial ligands. As a result of their axial ligation, they characteristically exhibit more intense ν_{11} bands which occur at lower energy ($\sim$1530$-$1540 cm^{-1}) relative to those of *c*-type hemes ($\sim$1545 cm^{-1}) (Kitagawa et al., 1977; Adar & Erecinska, 1974). Separation of the individual b_H and b_L spectra reveals that the two *b*-type hemes are quite distinctive. While the positions of the ν_{19} bands, and thus the heme core size are the same, the position and relative intensity of ν_{11} differ markedly for the two *b*-hemes. Heme b_H exhibits a ν_{11} band ($\sim$1536 cm^{-1}) similar to that of cytochrome b_5 ($\sim$1538 cm^{-1}) (Adar & Erecinska, 1974; Hobbs et al., 1990), while b_L has an anomalously lower energy ν_{11} even for *b*-type hemes. In fact, the position of ν_{11} for heme b_L ($\sim$1528 cm^{-1}) is approximated only by iron protoporphyrin bis(imidazole) complexes [Fe(II)PP(ImH)$_2$] where one or both of the ligands are deprotonated (Desbois & Lutz, 1992).

A comprehensive study of protoporphyrin model complexes by Debois and Lutz (1992) revealed a systematic correlation between heme modes and imidazole protonation states. ν_{11} was found to be extremely sensitive to this phenomenon, shifting from 1533 to 1526 to 1517 cm^{-1} for the Fe(II)PP(ImH)$_2$, Fe(II)PP(ImH)(Im$^-$), and Fe(II)PP(Im$^-$)$_2$ species, respectively. The Q- and B-band absorption spectrum of Fe(II)PP(ImH)$_2$ complexes also showed a red shift on ligand deprotonation. In addition, the deprotonation of the ligands can also be expected to decrease the heme redox potential substantially. Thus, we conclude that the anomalous spectra behavior of heme b_L most likely arises from the deprotonation (or strong hydrogen bonding) of at least one of its histidine ligands. A scenario where heme b_L exists as a heme(ImH)$_2$ $\rightleftharpoons$ heme(ImH)(Im$^{\delta-}\cdots$H$^{\delta+}$) equilibrium readily explains the extremely low frequency ν_{11}, the split Q_{00} absorption band and the low redox potential of heme b_L. As the pK_a of the histidine ImH $\rightleftharpoons$ Im$^-$ equilibrium is $>$14 (Moore & Pettigrew, 1990), heme exposure to solvent conditions cannot produce the observed effects. Instead, the local protein environment of heme b_L must be poised to lower the pK_a of at least one of the axial imidazoles and supply a nearby strong nucleophile (perhaps Asp, Arg, or Lys). It is tempting to speculate that this putative mechanism for proton abstraction could also provide a direct means of coupling electron transfer and proton pumping within the bc_1 complexes.

Allosteric interactions among hemes have been observed in many different classes of multiheme proteins. The data obtained in this study can be used to probe the existence of similar phenomena in bc_1 complexes. Isolated RR spectra can be generated for heme b_H in either the fully reduced and ascorbate reduced ("aged") bc_1 complexes (data not shown). These spectra can, in turn, be used to assess the degree to which the ferrous heme b_H local environment is sensitive to the redox state of heme b_L. Our data indicate that, at least under our experimental conditions, the heme b_H spectrum is unaffected by changing the heme b_L redox state. These findings are consistent with the lack of electronic and redox coupling between the two hemes and suggest direct interactions between ferrous hemes b_H and b_L are minimal.

(II) Effects of Inhibitor Binding

Resonance Raman spectroscopy was used to probe whether or not the binding of electron transfer inhibitors to bc_1 complexes produced any structural perturbations of the heme active sites. Both Q_i and Q_o inhibitors were used in this investigation.

Table 3: Q-Band RR Modes for Fully Reduced *Rb. capsulatus* bc_1 Complex and c_1 Subunit

	raw spectra				isolated heme spectra		
mode	c_1, 550 nm	bc_1, 550 nm	bc_1, 560 nm	bc_1, 565 nm	c_1	b_H	b_L
$\delta_{(CH=)}$ (cm^{-1})		1302	1302	1302		1301	1302
ν_{21} (cm^{-1})	1316	1316	1316		1315		
$\delta_{(=CH_{2(2)})}$ (cm^{-1})		1339	1339	1339		1339	1340
$\delta_{(CH_3)}$ (cm^{-1})	1363	1363	1363	1363	1363	1364	1363
ν_{20} (cm^{-1})	1397	1395	1393	1390	1397	1395	1390
ν_{11} (cm^{-1})	1543	1543	1537	1533	1543	1536	1528
ν_{19} (cm^{-1})	1586	1586	1586	1586	1586	1586	1586
ν_{10} (cm^{-1})	1624	1624	1623	1622	1624	1623	1622

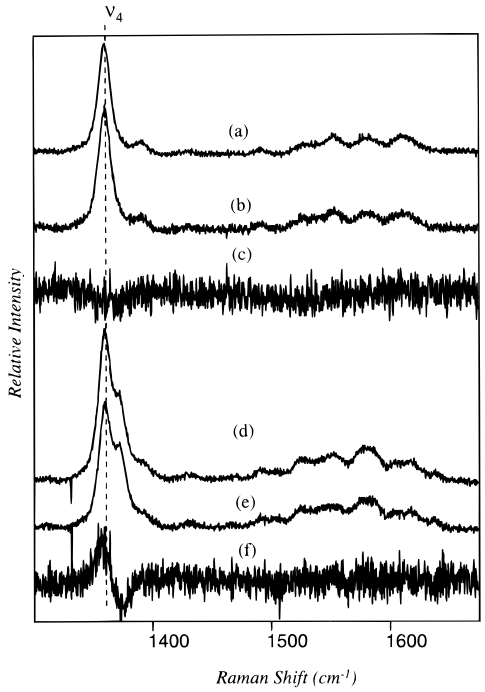

FIGURE 5: Raman difference spectra (baseline-corrected) of bc_1 complexes ± antimycin spectra. (a) Fully reduced bc_1 + antimycin, (b) fully reduced bc_1, no antimycin, (c) difference spectrum [(a) − (b)], (d) ascorbate-reduced bc_1 complexes + antimycin, (e) ascorbate-reduced bc_1 complexes, no antimycin, (f) difference spectrum [(d) − (e)]. Pairs of spectra were simultaneously obtained from sample in a customized rotating split cell. Samples were degassed with N_2 in a glove bag, and inhibitor or blank solvent (DMSO) was added under anaerobic conditions immediately before measurement. Final sample solution was ∼30 μM bc_1 complexes in 50 mM Tris-HCl (pH 8.0), 100 mM NaCl, 0.1 mg/mL dodecyl maltoside, ∼5% (v/v) DMSO, and 50 μM antimycin (where applicable). Laser power was 20−50 mW at 406 nm. Spectra are the sums of 2−3 scans at 25 cm^{-1}/min.

Antimycin is representative of inhibitors that block electron flow to the Q_i site (Link et al., 1993; Gennis et al., 1993). Figure 5 summarizes the results of our B-band RDS investigation of the effects of antimycin binding. This study proved challenging for several reasons. As the isolation of individual heme spectra was impossible with B-band excitation, Raman difference spectroscopy was employed to detect any shifts in the composite resonance Raman bands. The relatively high power continuous wave excitation required for this experimental protocol produced extensive photoreduction of the fully oxidized bc_1 complexes, which obscured any changes produced by antimycin binding. Reasonable spectra were, however, obtained for dithionite- and sodium ascorbate-reduced bc_1 samples in the presence and absence of antimycin.

Spectra of the complete high-frequency region of fully reduced bc_1 complexes with and without bound antimycin (Figure 5) show that inhibitor binding produces no dramatic alteration of the composite heme spectrum. It is clear that none of the hemes in the protein undergoes a change in spin state or axial ligand. RDS of both the fully (dithionite) and partially (ascorbate) reduced bc_1 complex reveals small differences in the composite ν_4 band. For the fully reduced bc_1 complexes, the RDS spectrum at ν_4 reveals a small structural perturbation of at least one of the reduced hemes upon antimycin binding. The partially reduced species exhibits two distinct bands at ν_4, reflecting the reduced hemes (c_1 and *a* fraction of b_H) and the oxidized hemes (b_L and remainder of b_H) at 1360 and 1372 cm^{-1}, respectively. The broad peak-to-trough separation in the difference spectrum almost surely arises from an increase in the net fraction of reduced heme in the plus antimycin sample. The independence of this phenomenon on laser power (data not shown) precludes photoreduction as the origin of the additional reduction. We spectulate that the increased relative intensity at ∼1360 cm^{-1} arises from a slight increase in b_H redox potential as a result of antimycin binding. Similar behavior has been observed in the absorption spectra of a mitochondrial bc_1 complex subsequent to antimycin binding (Howell & Robertson, 1993).

RR spectra obtained with Q-band excitation are much less ambiguous concerning the effects of antimycin binding. Figure 6 shows the raw spectra obtained from bc_1 complexes with and without the bound inhibitor, using various excitation wavelengths within the Q_{00} absorption band. Here again it is clear that none of the hemes undergo dramatic structural perturbation upon antimycin binding. However, careful subtraction of calibrated spectra reveals systematic changes in spectra obtained in resonance with the *b*-heme absorption (560 and 565 nm) that are largely absent in the 550-nm excitation data: a complex difference pattern is seen in the 1500−1650-cm^{-1} region, which apparently involves ν_{11}, ν_{21}, ν_{19}, and ν_{10}. Smaller changes are also apparent in a slight increase in the intensity of the weak band at ∼1450 cm^{-1} and shifts in the vinyl modes (∼1300 cm^{-1}).

It is clear that antimycin binding produces virtually no perturbation of the c_1 spectra and has a much smaller effect on the b_L than the b_H spectra. In fact, the separated b_H difference spectra (data not shown) obtained with 560-nm excitation yield a nearly identical pattern to that obtained from the composite spectra at that same excitation wavelength. This strongly suggests that small structural perturbations of b_H are the origin of most, if not all, of the spectral changes induced by antimycin binding to bc_1 complexes. These results are quite consistent with previous biochemical and mutagenesis investigations which indicate that the Q_i

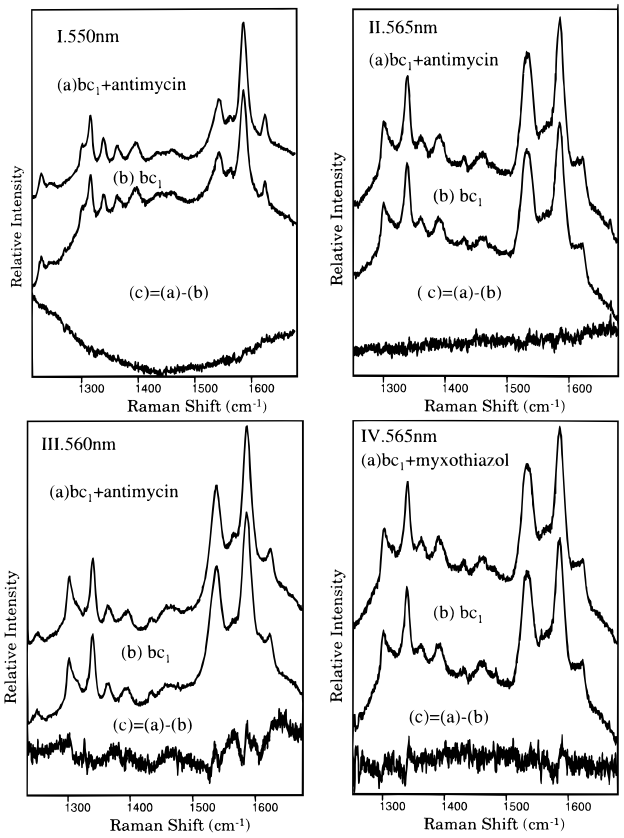

FIGURE 6: Q-band RR spectra of ferrous bc_1 complexes with and without inhibitors obtained at various excitation wavelengths. Panels I−III: (a) denotes spectra obtained from samples with antimycin, (b) denotes control spectra (ethanol but no antimycin), and (c) denotes their difference spectra. Panel IV: (a) spectrum from samples with myxothiazol, (b) control spectrum, (c) the difference spectrum, (a) − (b). Sample conditions are the same as Figure 3 with final concentrations of ∼140 μM bc_1, 5−6% (v/v) ethanol, and ∼250 μM antimycin or myxothiazol. All other experimental conditions were the same as those for Figure 3.

site is proximal to heme b_H. They further suggest that Q_i inhibitors do not bind in a manner that significantly displaces amino acid residues in direct contact with heme b_H. The small structural changes that are propagated to heme b_H apparently influence both the heme periphery (as reflected in the vinyl modes) and its ligation geometry (as reflected in ν_{11}, ν_{19}, and ν_{10}). It should be noted that those results pertain only to the ferrous hemes. In this regard, they complement earlier EPR studies of inhibitor bindings by Yu and co-workers (McCurley et al., 1990), which detected small perturbations of ferric heme b_H and heme b_L upon antimycin and myxothiazol binding, respectively.

Similar studies of myxothiazol binding were complicated by two factors: (1) lack of independent spectroscopic verification of the degree of inhibitor binding and (2) the instability of the sample under experimental conditions. The effects of sample instability were minimized by using fresh samples and limiting their exposure to laser excitation. Nonetheless, these spectra must be considered to be less quantitatively reliable than the antimycin binding data. There are, however, some qualitative trends in the spectra that are worthy of note. Like antimycin binding, the effects on the 550-nm excitation spectra (data not shown) produced by myxothiazol are minimal. This suggests that the local environment of heme c_1 is unaffected by the presence of an inhibitor at the Q_0 site. More pronounced effects are evident in the spectra dominated by *b*-heme scattering; in this case, however, the differences produced by myxothiazol are greater in spectra obtained with 565-nm excitation (Figure 6, panel IV), suggesting that the effects of Q_0-site inhibitors are most evident at heme b_L. These results are consistent with the widely accepted picture that the Q_0 binding site lies closer to heme b_L than to heme b_H.

SUMMARY AND CONCLUSIONS

This study represents the first quantitative resonance Raman investigation of the individual heme active sites of bc_1 complexes. The isolation and characterization of the vibrational spectra of heme c_1, b_H, and b_L are a necessary first step toward utilizing the structural sensitivity of RR scattering for the time-resolved investigation of the dynamics associated with the physiological functions of the complex. In addition, several useful conclusions can be drawn from the results of these initial investigations: (1) While B-band RR heme spectra are extremely difficult to separate, the differences in Q-band absorption among hemes c_1, b_H, and b_L allow for the isolation of their spectra using resonance selectivity and difference techniques. (2) The isolated RR Q-band spectra reveal that heme c_1 and b_H have "typical" *c*-type and *b*-type vibrational spectra, respectively. In contrast, heme b_L exhibits an anomalous RR spectrum, particularly for the axial ligand sensitive mode, ν_{11}. The extremely low energy (relative to other hemes *b*) of this mode and the low redox potential of heme b_L may be a reflection of protein-induced deprotonation (or strong hydrogen bonding) of at least one of the heme b_L histidine axial ligands. (3) Heme c_1 appears to be structurally isolated both from the other hemes and from effects of inhibitor binding at the Q_i site of the complex. (4) There is no evidence in the RR spectra for direct structural communication between the *b*-hemes. In particular, the local environment of ferrous heme b_H is unaffected by the redox state of heme b_L. (5) Neither Q_i nor Q_0 inhibitors produce dramatic structural changes at the *b*-hemes upon binding to the complex. In particular, the anomalous ligation environment of heme b_L is not dramatically changed by the binding of inhibitors. Antimycin binding does induce minor changes in the heme b_H environment, while myxithiozal binding produces similarly small perturbations of heme b_L.

ACKNOWLEDGMENT

We thank Dr. F. Daldal for his generous donation of the bc_1 overproducing strain of *Rhodobacter capsulatus* used in these studies, Dr. K. A. Gray for his advice on c_1 isolation, and Drs. M. K. Johnson and D. E. Robertson for helpful discussions.

REFERENCES

Adar, F., & Erecinska, M. (1974) *Arch. Biochem. Biophys. 165*, 570−580.
Babcock, G. T. (1988) in *Resonance Raman Spectra of Heme and Metalloproteins* (Spiro, T. G., Ed.) Academic Press, New York.
Babcock, G. T., & Varotsis, C. (1993) *J. Bioenerg. Biomembr. 25*, 71−80.
Beattie, D. S., Jenkins, H. C., & Howton, M. M. (1994) *Arch. Biochem. Biophys. 312*, 292−300.
Brandt, U., & Trumpower, B. L. (1994) *Crit. Rev. Biochem. Mol. Biol. 29*, 165−197.
Carter, K. R., Tsai, A., & Palmer, G. (1981) *FEBS Lett. 132*, 243−246.

Chen, Y. R., Shenoy, S. K., Yu, C. A., & Yu, L. (1995) *J. Biol. Chem. 270*, 11496−11501.
Crofts, A. R., & Wang, Z. (1989) *Photosynth. Res. 22*, 68−87.
Daldal, F., Tokito, M. K., Davidson, E., & Faham, M. (1989) *EMBO J. 8*, 3951−3961.
Davidson, E., & Daldal, F. (1987) *J. Mol. Biol. 195*, 13−24.
Davidson, E., Ohnishi, T., Tokito, M., & Daldal, F. (1992) *Biochemistry 31*, 3351−3358.
Desbois, A. (1994) *Biochimie 76*, 693−707.
Desbois, A., & Lutz, M. (1992) *Eur. Biophys. J.* 321−335.
Finnegan, M. G., Knaff, D. B., Qin, H., Gray, K. A., Daldal, F., Yu, L., Yu, C., Kleis-San Francisco, S., & Johnson, M. K. (1996) *Biochim. Biophys. Acta 1274*, 9−20.
Gennis, R. B., Barquera, B., Hacker, B., Van Doren, S. R., Arnoud, S., Crofts, A. R., Gray, K. A., & Daldal, F. (1993) *J. Bioenerg. Biomembr. 25*, 195−209.
Gouterman, M. (1978) in *The Porphyrins. III. Physical Chemistry, Part A* (Dolphin, D., Ed.) Academic Press, New York.
Gray, K. A., Davidson, E., & Daldal, F. (1992) *Biochemistry 31*, 11864−11873.
Guper, S., Willie, A., Millett, F., Caffrey, M. S., Cusanovich, M. A., Robertson, D. E., & Knaff, D. B. (1993) *Biochemistry 32*, 4793−4800.
Hauska, G., & Herrmann, R. G. (1988) *J. Bioenerg. Biomembr. 20* (2), 211.
Hauska, G., Hurt, E., Gabellini, N., & Lockau, W. (1983) *Biochim. Biophys. Acta 726*, 97−133.
Hobbs, J. D., Kriaucuunas, A., Guner, S., Knaff, D. B., & Ondrias, M. R. (1990) *Biochim. Biophys. Acta 1018*, 47−54.
Howell, N., & Robertson, D. E. (1993) *Biochemistry 32*, 11162−11172.
Hu, S., Morris, I. K., Singh, J. P., Smith, K. M., & Spiro, T. G. (1993) *J. Am. Chem. Soc. 115*, 12446−12458.
Kitagawa, T., Ozaki, Teraoka, J., Kyogoku, Y., & Yamanaka, T. (1977) *Biochim. Biophys. Acta 494*, 100−114.
Knaff, D. B. (1993) *Photosynth. Res. 35*, 117−133.
Kunz, W. S., & Konstantinov, A. A. (1983) *FEBS Lett. 152* (1), 53.
Link, T. A., Haase, U., Brandt, U., & von Jagow, G. (1993) *J. Bioenerg. Biomembr. 25*, 221−232.
Lou, B., Hobbs, J. D., Chen, Y., Yu, L., Yu, C., & Ondrias, M. R. (1993) *Biochim. Biophys. Acta 1144*, 403−409.
McCurley, J. P., Miki, T., Yu, L., & Yu, C. (1990) *Biochim. Biophys. Acta 1020*, 176−186.
Mitchell, P. (1976) *J. Theor. Biol. 62*, 327−367.
Moore, G. R., & Pettigrew, G. W. (1990) *Cytochromes c. Evolutionary, Structural and Physicochemical Aspects*, Springer-Velag, Berlin.
Othman, S., Le Lirzin, A., & Desbois, A. (1994) *Biochemistry 33*, 15437−15448.
Otsuka, S., & Yamanaka, T. (1988) *Metalloproteins, Chemical Properties and Biological Effects*, Kdansha Ltd., Tokyo.
Rich, P. R., Jeal, A. E., Madgwich, S. A., & Moody, A. J. (1990) *Biochim. Biophys. Acta 1018*, 29−40.
Robertson, D. E., Farid, R. S., Moser, C. C., Urbauer, J. L., Mulholland, S. E., Pidikiti, R., Lear, J. D., Wand, A. J., DeGrado, W. F., & Dutton, P. L. (1994) *Nature 368*, 425−432.
Rousseau, D. L., & Friedman, J. M. (1988) in *Resonance Raman Spectra of Heme and Metalloproteins* (Spiro, T. G., Ed.) Academic Press, New York.
Shelnutt, J. A., Rousseau, D. L., Dethmers, J. K., & Margoliash, E. (1981) *Biochemistry 20*, 6485−6497.
Simpkin, D., Palmer, G., Devlin, F. J., Mckenna, M. C., Jensen, G. M., & Stephens, P. J. (1989) *Biochemistry 28*, 8033−8039.
Slater, E. C. (1973) *Biochim. Biophys. Acta 301*, 129−154.
Spiro, T. G., & Li, S. (1988) in *Resonance Raman Spectra of Heme and Metalloproteins* (Spiro, T. G., Ed.) Academic Press, New York.
Takahashi, S., Wong, J., Rousseau, D. L., Ishikawa, K., Yoshida, T., Takeuchi, N., & Ikeda-Saito, M. (1994) *Biochemistry 33*, 5531−5538.
Trumpower, B. L. (1990) *J. Biol. Chem. 265*, 11409−11412.
Yun, C. H., Crofts, A. R., & Gennis, R. B. (1991) *Biochemistry 30*, 6747−6754.
Yun, C. H., Wang, Z., Crofts, A. R., & Gennis, R. B. (1992) *J. Biol. Chem. 267*, 5901−5909.

BI960419V